Loss Evaluation of a Two-stage Boost Converter Using the Neutral Point of a Motor

Jun-ichi Itoh
Member, IEEE
Nagaoka University of Technology
1603-1 Kamitomioka-cho Nagaoka City
Niigata, Japan
itoh@vos.nagaokaut.ac.jp

Daisuke Ikarashi
Student Member, IEEE
Nagaoka University of Technology
1603-1 Kamitomioka-cho Nagaoka City
Niigata, Japan
dai1446@stn.nagaokaut.ac.jp

***Abstract* -- This paper evaluates the loss of the proposed two-stage boost converter using the neutral point of a motor, which consists of a small boost chopper and a three-phase inverter. The proposed converter uses the leakage inductance of a motor instead of an ordinary boost-up reactor as a passive boost up component. However, the DC current is imposed to the phase current of the motor in the proposed circuit. Thus the proposed circuit is difficult to separate the power loss between the motor part and the inverter part. The basic operation of the proposed circuit is confirmed by experimental results. In additionally, a measurement method of a power loss in each part of the proposed circuit is established and demonstrated in the test circuit. The efficiency of the boost converter stage of the proposed circuit is increased by 2.3% in compared to the conventional circuit.**

***Index Terms*—DC-DC power conversion, DC-AC power conversion, Pulse width modulated inverters, Permanent magnet motors, Motor drives, Inductance, Loss measurement**

I. INTRODUCTION

Recently, motor drive technologies that drive with a battery are highly demanding in a lot of applications such as electric vehicles and rail trains [1]. In order to obtain high efficiency, high terminal voltage at the motor is needed. However, a higher voltage needs to increase the volume of the battery bank and results an increase in term of cost. Therefore, the battery is usually connected to a boost converter before an inverter.

Fig. 1 shows the conventional DC-AC power converter, which is composed of batteries, a boost converter and a three-phase inverter. Battery voltage is increased by the boost converter when the inverter outputs high voltage to the motor. However, the boost converter requires a large boost-up reactor, which is high cost and bulky. In addition, higher switching frequency is applied in order to reduce the volume of the boost-up reactor; however this strategy will increase the switching losses. One of solutions to reduce the switching losses under high frequency, resonance converters are used [2-4]; however this method increased the number of components in the boost-up converter.

In order to solve this problem, the authors have been proposed a reactor free boost-up converter that uses the leakage inductance of a motor instead of a boost-up reactor [5-6].

Fig. 2 shows the DC/AC conversion reactor free boost-up converter [6-7]. In the proposed converter, the neutral point of a motor is connected to a battery directly. So, the proposed converters can increase the inverter output voltage without increasing the number of components.

However, the proposed converter is having two problems. First, the maximum peak value of the inverter output phase voltage is limited by the battery voltage. Therefore, when the boost-up ratio is two times higher and above, the modulation factor of the inverter will be decreased.

Fig. 3 shows the controllable range of fig. 2. Second, the six-step modulation can not be applied to the proposed converter. In the six-step modulation, the neutral point voltage of a motor will fluctuate at a frequency which is three times of the output frequency. Since the battery is connected to the neutral point of the motor, the input current will contain large ripple due to the fluctuation of the neutral point voltage of the motor. Therefore, another small boost-up stage is proposed to connect to the neutral point of a motor [8].

This paper evaluates the loss of the proposed two-stage converter in order to optimize the motor design and power converter design. Especially, the proposed circuit generates the motor and inverter loss by zero-phase current where the DC current of the battery is added to the phase current of the motors in the proposed circuit. Thus the proposed circuit is difficult to separate the motor part and the inverter part into two items for power loss measuring. This paper describes a measurement method of a power loss in each part of the proposed circuit. The validity of the measurement method is confirmed by the simulation and the experiment. Furthermore, the loss distribution of the proposed system is demonstrated in the test circuit. A power loss in each part of the proposed circuit is measured and compared with the conventional circuit. In additionally, the basic operation of the proposed circuit is confirmed by experimental results.

II. CIRCUIT TOPOLOGY

A. Circuit configuration

Fig. 4 shows the proposed circuit configuration. The proposed circuit is composed of batteries, a three-phase inverter and a first stage boost converter that connects to the neutral point of a motor. The inverter in the proposed circuit comes with a boost-up function when the motor leakage inductance is utilized. However, the DC current is imposed to the phase current of the motor in the proposed circuit.

The proposed circuit can reduce the volume of the boost-up reactor and switching losses in the first stage boost converter. When a sinusoidal wave triangle carrier comparison method is used to generate PWM pulses, the neutral point voltage of the motor is the same as the neutral point voltage of the DC link part, i.e. half of the DC link voltage E_{dc1}. Therefore, the rating voltage of the boost-up reactor and switching device in the first stage boost converter is reduced to the half of DC link voltage. It should be noted that the capacitor C_2 that is connected to the neutral point of the motor is 100 times smaller than the DC link capacitor C_1 of the inverter.

The applied voltage of the boost-up reactor assumes to be constant during a switching cycle. So, the relations between the inductance of boost-up reactor L and the input current ripple ΔI_{in} can be expressed as

$$\Delta i_{in} = \frac{1}{L}\int_0^{d/f_{sw}} v_L dt = \frac{v_L d}{L f_{sw}} \quad (1)$$

where the d is duty ratio, f_{sw} is the switching frequency, v_L is the applied voltage of reactor.

When the input current ripple ΔI_{in} is designed, the required inductance of the boost-up reactor L is derived from equation (1).

Fig. 5 shows the relationship between the boost-up ratio and the reduction ratio of inductance in the proposed circuit. When the boost-up ratio is 3, the proposed circuit can reduce the inductance of boost-up reactor by half as compared to the conventional circuit. Therefore, the proposed circuit can reduce the size of boost-up reactor.

B. Positive phase sequence equivalent circuit

Fig. 6 shows the positive-phase sequence equivalent circuit. The proposed circuit can be divided between the positive and negative sequence components. The boost converter does not appear in the positive-phase sequence equivalent circuit due to the connection of the neutral point of the motor. Consequently the positive-phase sequence equivalent circuit is similar to a conventional three-phase inverter. During the PWM control, when the sinusoidal modulation is based on the triangle carrier comparison to generate PWM pulses, the fundamental voltage of the output is given by (2)

$$V_{out} = \frac{\sqrt{3}}{2\sqrt{2}} E_{dc} \cdot a \quad (2)$$

where V_{out} is the output line voltage, E_{dc} is the DC link voltage and a is the modulation index.

In the proposed circuit, a six-step operation is applied to the three-phase inverter in order to reduce the switching loss of the inverter in comparison to a PWM inverter. During the

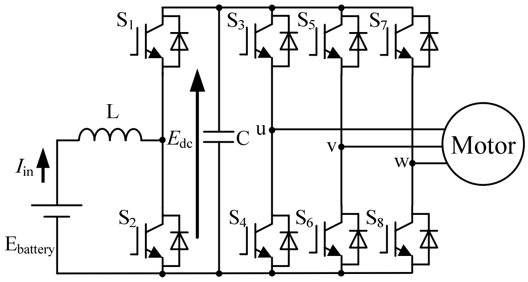

Fig. 1. Conventional circuit diagram

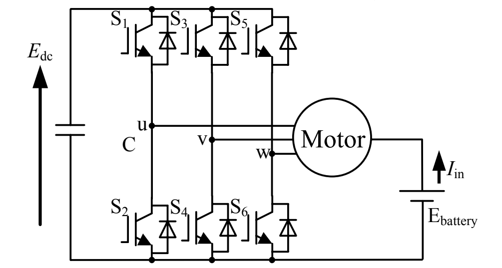

Fig. 2. DC/AC conversion reactor free boost-up converter

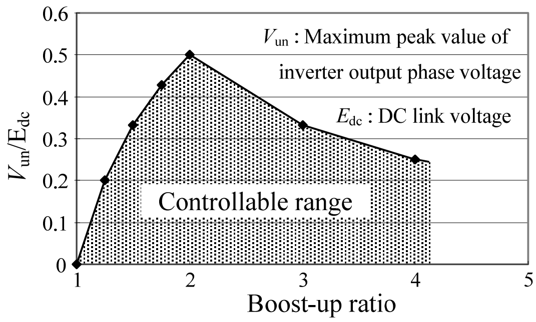

Fig. 3. Controllable range of fig. 2

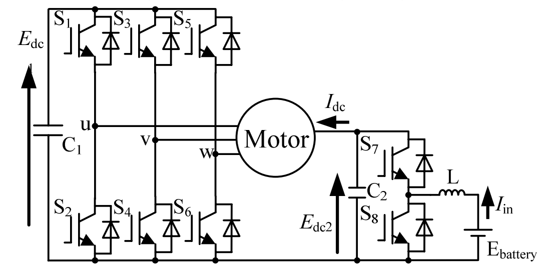

Fig. 4. Proposed circuit diagram

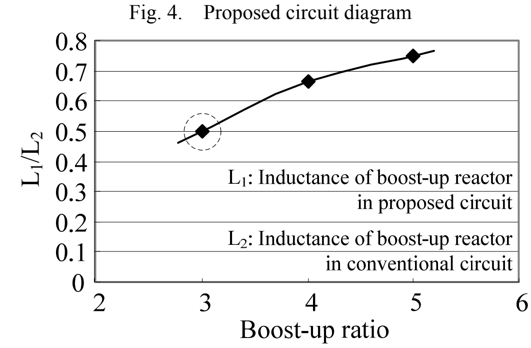

Fig. 5. The relationship between the boost-up ratio and the reduction ratio of inductance in the proposed circuit

six-step operation, the switching frequency agrees with the output frequency. The output line voltage becomes a 120 degree square waveform, then, the fundamental voltage of the output is given by (3)

$$V_{out} = \frac{\sqrt{6}}{\pi} E_{dc} \quad (3)$$

where V_{out} is output line voltage, E_{dc} is the DC link voltage.

C. Zero phase sequence equivalent circuit

Fig. 7 shows the zero-phase sequence equivalent circuit. The back electromotive force (EMF) does not appear in the zero-phase sequence equivalent circuit but only the leakage inductance exists. In zero-phase sequence, the inverter legs could consider to a single leg. Then the output voltage of the single leg is the same as the neutral point voltage of the motor. A two-stage boost up operation is achieved by two choppers, which are constructed by switch S_1, S_2 and switch S_3 and S_4. However, the leakage inductance of the motor decreases to 1/3 since the leakage inductance of the motor is connected in parallel in the zero-phase sequence equivalent circuit.

On the other hand, the neutral point voltage of the motor is given by (4)

$$E_{dc2} = \frac{1}{3}(v_u + v_v + v_w) + \frac{1}{2} E_{dc1} \quad (4)$$

where E_{dc2} is the neutral point voltage of the motor, v_u, v_v and v_w are the motor phase voltage and E_{dc1} is the DC link voltage.

Therefore, the neutral point voltage of the motor can be controlled by the zero-phase voltage command. In particular, the average of the neutral point voltage of the motor for one switching period is zero when the symmetrical three-phase sinusoidal waveform is used as modulation signal. Therefore the neutral point voltage of the motor equals to double of the DC link voltage. Furthermore, sum of the maximum inverter output voltage command and the zero-phase voltage command is limited by the neutral point voltage of the motor. If the battery connects the neutral point of the motor directly, the maximum phase voltage of the motor is constrained by the battery voltage. However in the proposed circuit, the maximum phase voltage is not constrained by the battery voltage because the neutral point voltage of the motor is controlled by the boost converter.

III. CONTROL STRATEGY

A. Control method of output voltage

Fig. 8 shows the control block diagram of the proposed circuit. The control of motor current in the proposed circuit is the same as a conventional three-phase inverter because the positive-phase sequence equivalent circuit is similar to a conventional three-phase inverter. The stabilization control is applied to achieve a V/f control for the permanent magnetic

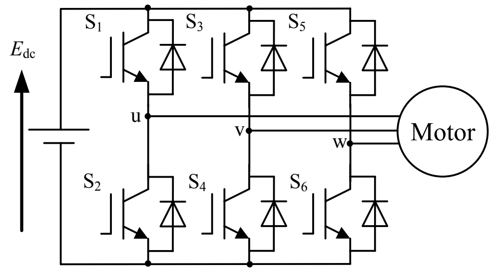

Fig. 6. Positive phase sequence equivalent circuit

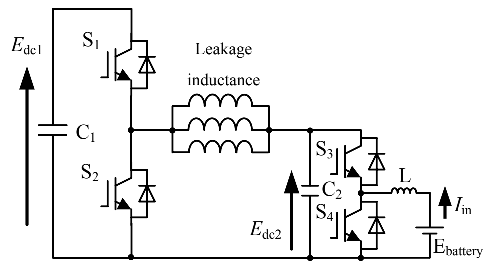

Fig. 7. Zero phase sequence equivalent circuit

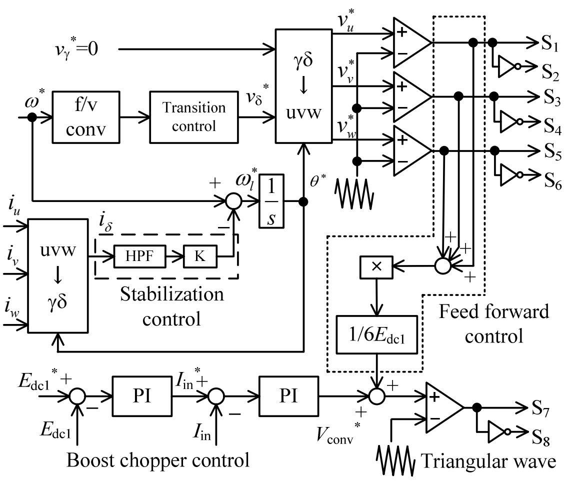

Fig. 8. Control block diagrams

motor [9]. Additionally, the PWM control is slowly changed into a six-step operation via the trapezoidal pulse modulation. The transition control in Fig.8 is a proportional compensation to the amplitude of the output voltage command because the output voltage is nonlinearly increasing at the trapezoidal pulse area [10].

B. Battery current compensation control

In the proposed circuit, when the six-step operation is applied to the inverter control, the input current is distorting at three times of the output frequency. This is because the neutral point voltage of the motor has fluctuation of $\pm 1/6E_{dc1}$ with three times of the inverter output frequency in the six-step operation. In order to compensate the voltage fluctuation, a feed forward control is applied to a current regulator in the first stage boost converter. The voltage fluctuation is estimated by the DC link voltage and the pulse pattern of the inverter.

IV. LOSS MEASUREMENT METHOD

Fig. 9 shows the power flow of the proposed circuit. In the proposed circuit, the motor losses by zero-phase current occur between the boost converter losses and the inverter losses because the neutral point of a motor is connected to a boost converter with a battery voltage as the input voltage. In consequence the inverter losses can not be calculated as the difference between the boost converter output power and the inverter output power merely. Therefore, it is difficult to separate the power loss between the motor part and the inverter part. However, the proposed circuit can be considered as one of the three-phase four wires system. Then the total power of the converter is measured by the sum of the instantaneous power of each phase.

Fig. 10 shows the method for measurement of the inverter losses. The inverter losses in the proposed circuit are given by (5) based on a four wires system.

$$P_{invloss} = v_1 i_1 + v_2 i_2 + v_3 i_3$$
$$= e_{dc2} i_{dc} - (v_u i_u + v_v i_v + v_w i_w) - \frac{i_{dc}}{3}(v_{R1} + v_{R2} + v_{R3}) \quad \text{.............} \quad (5)$$

where v_u, v_v and v_w are positive-negative phase instantaneous voltage, i_u, i_v and i_w are positive-negative phase instantaneous current.

V. SIMULATION RESULTS

In order to demonstrate the loss distribution of the proposed system, the loss is analyzed by the simulation. The converter loss analysis was implemented by a circuit simulator (PSIM, *Powersim Technologies Inc.*) and DLL files (Dynamic Link Library) [11]. The converter losses are estimated by the applied voltage for the switching device, the collector current and the characteristics of the data sheet. The circuit uses IGBT (2MBI50N-060), the rated collector-emitter voltage is 600 V and the rated collector current is 50A. It should be noted that in the converter loss analysis, the loss of a boost-up reactor is neglected. The motor loss is analyzed in a 2D finite element method (FEM) by simulating a 1.5-kW interior permanent-magnet motor.

Table 1 shows the internal permanent magnet (IPM) motor parameters. The motor phase current of the conventional system is assumed as sinusoidal current without the DC current. By contrast, the proposed system condition is with the DC current, where the DC current is −4.0A per single phase.

Fig. 11 shows a total efficiency comparison between the proposed system and the conventional system during the PWM control. The efficiency of the proposed system is lower than the conventional system approximately 3% because the copper loss of the motor is increased 30% by the zero-phase current. In contrast, the switching loss of the boost converter in the proposed circuit is decreased by half. So, the proposed circuit can increase the converter efficiency.

Fig.12 shows a total loss analysis comparison between the proposed system and the conventional system during the

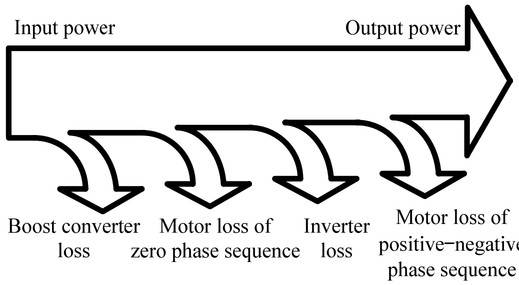

Fig. 9. Power flow of the proposed circuit

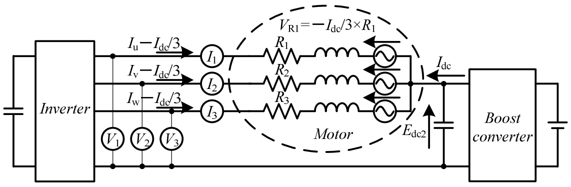

Fig. 10. Method for measurement of the inverter losses in the proposed circuit

TABLE I
IPM MOTOR PARAMETERS

Motor Power	1.5kW
Rated Voltage	180V/phase
Rated Current	6.1A
Rated Speed	1800rpm
Number of Poles	6poles
Number of Stator Slots	36slots
Stator Outer Diameter	130mm
Stator Inner Diameter	83mm
Winding Configuration	138turn,series per phase
Rotor Outer Diameter	82.2mm
Rotor Shaft Diameter	30mm

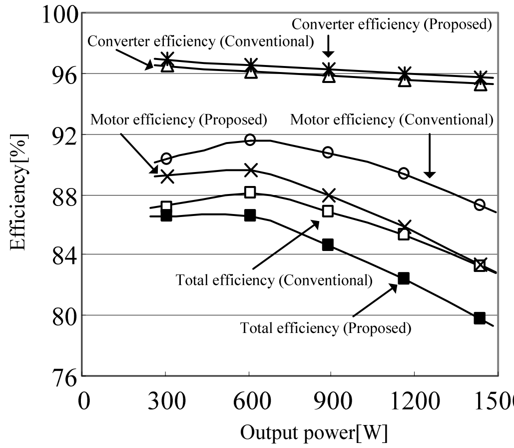

Fig. 11. Total efficiency comparison of the proposed system with the conventional system

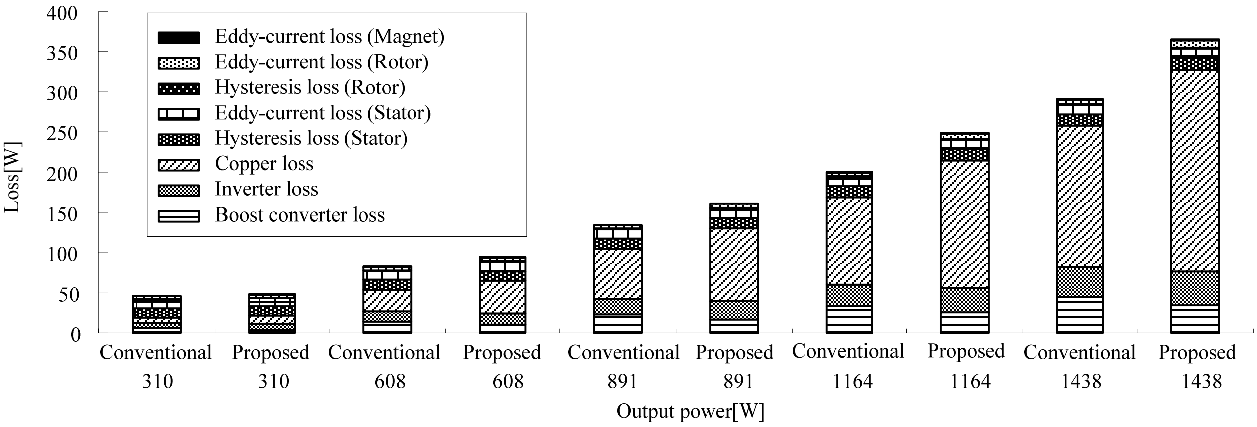

Fig. 12. Total loss analysis in simulation

PWM control by applying 5 difference load conditions. The total loss of the motor drive system that drive with a battery is consist of a boost converter loss, a three-phase inverter loss, a copper loss of motor and an iron loss of motor. The loss simulation estimates that the proposed circuit can reduce the boost converter loss by 20% as compared to the conventional circuit because the proposed circuit can reduce the terminal voltage of the boost converter. However, the conduction loss in the inverter is increased by the zero-phase current.

Furthermore, the copper loss of the motor is increased by the DC current components because the copper loss is proportional to the square of the motor current. On the other hand, the iron loss caused by zero-phase current is very low.

Fig. 13 shows the magnetic field analysis results in simulation. Fig. 13(a) shows the line of magnetic flux where the motor model contains sinusoidal three-phase current only. Fig 13(b) shows the line of magnetic flux where the motor model contains only DC current. In the Fig 13(b), the main flux of the DC current is denied with each other. Therefore, the DC current excites only a leakage flux. So, the zero-phase current in the motor does not generate motor torque [12].

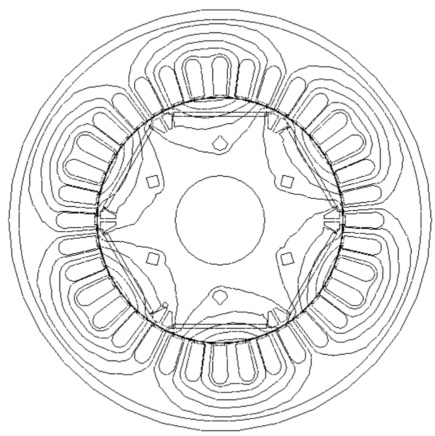

(a) The magnetic flux for sinusoidal three-phase current

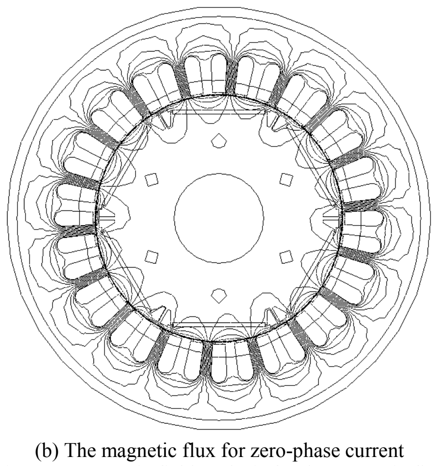

(b) The magnetic flux for zero-phase current

Fig. 13 Magnetic field analysis for the magnetic flux

VI. EXPERIMENTAL RESULTS

The proposed system was tasted in the prototype circuit. Table 2 shows the experimental parameters, the IPM motor is 750 W, 175 V and 90 Hz, and the battery voltage is 70 V. In this experiment, the output torque is controlled to 100%.

Fig.14 shows the operation waveforms during a PWM control of the inverter. In Fig. 14, the DC link voltage E_{dc1} is increased to twice of the neutral point voltage E_{dc2} by the inverter side boost-up function. Furthermore the DC link voltage E_{dc1} is controlled to 286 V by a voltage regulator. On the other hand, the motor current contains the DC components because the motor current is added with the zero-phase current. However, the sinusoidal motor current waveform and sinusoidal line voltage of the motor are obtained. It should be noted that the output line voltage V_{uv} is observed by using a low-pass filter of 1.5 kHz cut-off frequency to observe the low frequency component distortion.

Fig. 15 shows the experimental result during a six-step operation. When the six-step operation is applied to the inverter control, the input current is distorting at a frequency of three times of the output frequency. However, Fig. 15 shows that the ripple in the input current has been suppressed by the proposed control. Furthermore, the DC link voltage is

TABLE II
EXPERIMENTAL PARAMETERS

Battery volatge $V_{battery}$	70[V]
Output frequency	90[Hz]
PM motor rated output	750[W]
Rated voltage	175[V]
Rated current	3.3[A]
Rated speed	1800[rpm]
Number of poles	6poles
Switching frequency	10[kHz]
Boost chopper reactor L	1.7[mH]
Zero phase inductance	1.9[mH]
Capacitor C_1	1100[μF]
Capacitor C_2	5.0[μF]

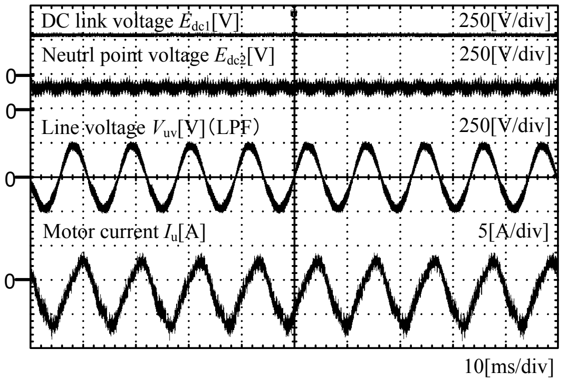

Fig. 14. Experimental results with PWM control

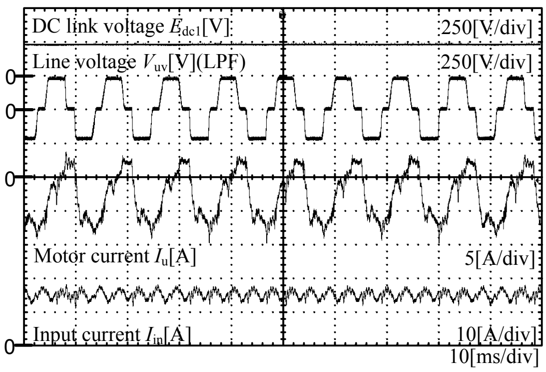

Fig. 15. Experimental results during six-step operation

controlled constant by the voltage regulator in the first stage boost converter.

Fig. 16 shows a converter loss comparison between the analysis results and the experimental results during a PWM control. The inverter loss in the proposed circuit is measured by the three-phase four-wire system. From fig. 16, notice that the analysis result is different from the experimental result at low power region. This is due to the no-load loss. So, when the converter outputs at the rated power, the error of loss analysis is about 15%. Meanwhile, it is confirmed that, the proposed circuit can reduce converter loss by 10% as compared to the conventional circuit at the rated operation because the proposed circuit can decrease the first stage boost

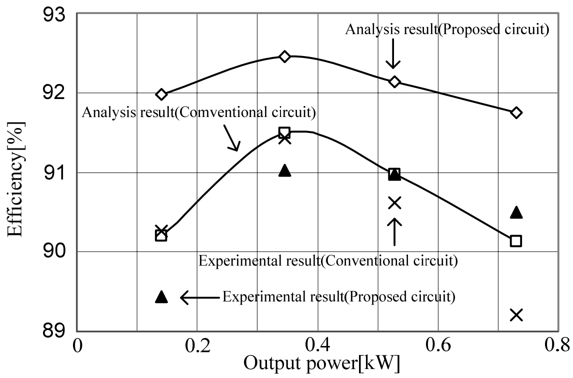

Fig.16. The converter efficiency comparison of the analysis results with the experimental results

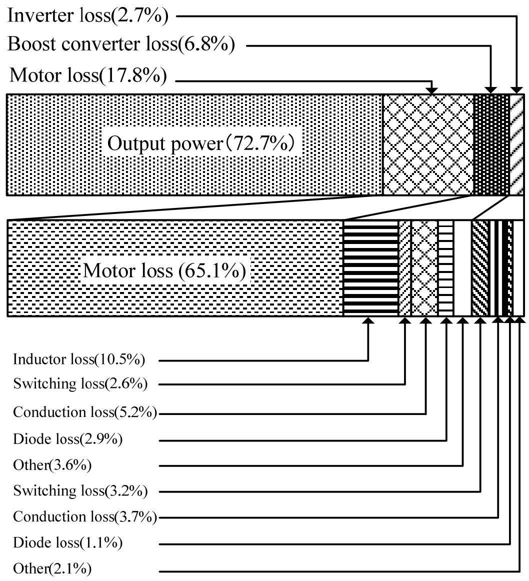

Fig. 17 Loss separation of the proposed system

converter loss.

Fig. 17 shows a loss separation result of the proposed system. The result shows that major loss is dominant by the motor loss in the proposed system. Especially in the proposed system, the copper loss of motor is large due to the zero-phase current. On the other hand, the loss in the boost-up reactor is dominant in the converter. Therefore, a reduction on the loss of the boost reactor loss is needed for obtaining high efficiency in the converter.

Fig. 18 shows the total loss comparison of the proposed system with the conventional system. The efficiency of the boost converter in the proposed circuit is increased by 2.3%. The efficiency is better because the applied voltage for the switching device in the boost converter decreases to less than 1/2 times in compared to the conventional circuit. Therefore, the switching loss in the boost converter is decreased by half. Similarly, the low voltage resistance switching device can be used in the first stage boost converter of proposed circuit.

Furthermore, the copper loss of the boost-up reactor can be decreased and the proposed circuit can reduce the size of the boost-up reactor to a half due to the low voltage terminal. However, the inverter losses and the motor losses are increased because the DC current is imposed into the phase current of the motor in the proposed circuit. In future, an optimization method on the motor is required in order to reduce the motor losses caused by zero-phase current.

VII. CONCLUSION

A novel two-stage DC-AC power converter connected to the neutral point of the motor has been proposed. The proposed circuit can reduce the volume of the boost-up reactor and switching losses in the boost converter. This paper discussed a measurement method of a power loss in each part of the proposed circuit. The measurement method of a power loss in each part of the proposed circuit is established and demonstrated in the test circuit. Then, the converter loss of the experimental result is compared to the analysis result. Furthermore, a power loss in each part of the proposed circuit is measured and compared with the conventional circuit. From the loss separation result, the efficiency of the boost converter of the proposed circuit is increased by 2.3% in compared to the conventional circuit. In additionally, the basic operation of the proposed circuit is confirmed by experimental results. A six-step operation is applied to the proposed converter with a feed forward control to compensate the fluctuation at the motor neutral point voltage. In future work, the motor will be optimized to reduce the loss that is caused by zero-phase current.

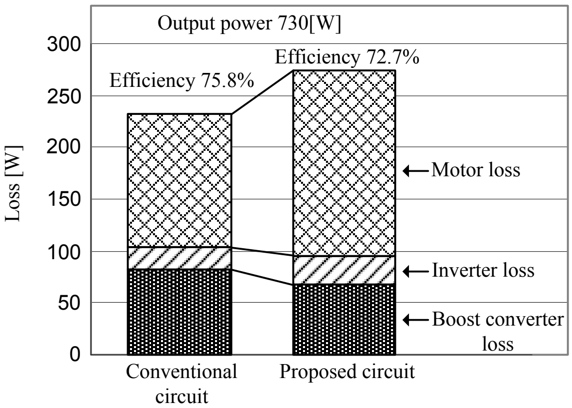

Fig. 18 Total loss comparison of the proposed system with the conventional system

REFERENCES

[1] Y.Tsuruta, and A.Kawamura, "Proposal of 98.5% High Efficiency Chopper Circuit QRAS for the Electric Vehicle and the Verification," Trans. IEEJ, Vol.125, No.11, pp.977-987, 2005.
[2] M.Yamamoto, S.Sato, E.Hiraki, and M.Nakaoka, "New Space Vector Modulated 3-Level 3-Phase Voltage-Source Soft-Switching Inverter with Two Active Resonant DC Link Snubbers," Trans. IEEJ, Vol.123-D, No.12, pp.1397-1405, 2003.
[3] S.Inasaka, A.Kawamura, Y.Tsuruta "Research for High Efficient Electrical Power Management apply Bilateral Chopper for Electric Vehicle," JIASC IEEJ, pp.I-667-I-670, 2009.
[4] S.Nagai, S.Sato, M.Yamamoto, E.Hiraki, M.Nakaoka "Effective Improvement of DC Busline Voltage Utilization Factor in Two Switch-Auxiliary Quasi-Resonant DC Link Snubber Assisted Three Phase Voltage Source Type Soft-Switching PWM Inverter," IEEJ Trans. Vol.123-D, No.6, pp.710-716, 2003.
[5] J.Itoh, and S.Ishii, "A Novel Single-phase High Power Factor Converter with Load Neutral Point Applied to PM Motor Drive," Trans. IEEJ, Vol.121-D, No.2, pp.219-224, 2001.
[6] T. Katagiri and J.Itoh: "PM motor driving with a boost type DC/AC conversion circuit using motor neutral point," Annual meeting of IEEJ, pp.142-143, 2007.
[7] K.Moriya, H.Nakai, Y.Inaguma and S.Sasaki "A DC/DC Converter Using Motor Neutral Point and its Control Method," Annual meeting of IEEJ, Vol.4, pp.119-120, 2004.
[8] J.Itoh, and D.Ikarashi, "Investigation of a Two-stage Boost Converter using the Neutral Point of a Motor," International Power Electronics Conf., ECCE ASIA, IPEC-Sapporo, pp.1189-1194, 2010.
[9] J.Itoh, J.Toyosaki, and H.Ohsawa, "High performance V/f control method for PM Motor," Trans. IEEJ, Vol.122-D,No.3 No.2 pp.253-259, 2002.
[10] N.Ohtani, J.Itoh "Square Wave Operation for a Single-phase PFC Three-phase Motor Drive System without a Reactor," The International Conference on Electrical Machines and Systems, LS4E-4, 2009.
[11] J.Itoh, and T.Iida, "Realization of High Efficiency AC Link Converter System Based on AC/AC Direct Conversion Techniques with RB-IGBT," IEEE Industrial Electronics Conf., Paris, pp.1703-1708, 2006.
[12] H.Plesko, J.Biela, J.Luomi and J.W.Kolar "Novel Concepts for Integrating the Electric Drive and Auxiliary DC-DC Converter for Hybrid Vehicles," IEEE Trans. Vol.23, No6, pp.3025-3026, 2008.